Science Advances
AAAS

advances.sciencemag.org/cgi/content/full/6/28/eabb5320/DC1

Supplementary Materials for

One-step vapor-phase synthesis of transparent high refractive index sulfur-containing polymers

Do Heung Kim, Wontae Jang, Keonwoo Choi, Ji Sung Choi, Jeffrey Pyun,
Jeewoo Lim*, Kookheon Char*, Sung Gap Im*

*Corresponding author. Email: sgim@kaist.ac.kr (S.G.I.); khchar@plaza.snu.ac.kr (K.C.); jeewoo@khu.ac.kr (J.L.)

Published 8 July 2020, *Sci. Adv.* **6**, eabb5320 (2020)
DOI: 10.1126/sciadv.abb5320

This PDF file includes:

Supplementary Text

X-ray reflectometry (XRR) analysis

The analysis method involves measuring the intensity of X-ray beam reflected on the sample with changing the incident angle of X-ray. In the XRR analysis, the refractive index of material can be estimated by the equation (1). When the incident angle is lower than the critical angle, incident X-ray beam is totally reflected and thus the reflectivity value becomes 1. Therefore, the critical angle is related to the refractive index of material, which can be calculated by the following equations *(38).*

$$n = 1 - \delta - i\beta \qquad (1)$$

$$\delta = \left(\frac{r_e \lambda^2}{2\pi}\right) N_o \rho \sum_i x_i (Z_i + f_i{}') / \sum_i x_i M_i \qquad (2)$$

$$\beta = \left(\frac{r_e \lambda^2}{2\pi}\right) N_o \rho \sum_i x_i (Z_i + f_i{}'') / \sum_i x_i M_i \qquad (3)$$

r_e: Classical radius of an electron (2.818×10^{-9} m); N_o: Avogadro number;

λ: X-ray wavelength; ρ: Density (g/cm^3); Z_i: Atomic number of the ith atom;

M_i: Atomic weight of the ith atom; x_i: Atomic ratio of the ith atom;

$f_i{}'$, $f_i{}''$: Atomic scattering factor of the ith atom

where δ is the energy dispersive term, and β is X-ray absorption term.

The real part of the complex refractive index is related to the phase velocity of X-ray in the material, and the imaginary part is related to the X-ray absorption of the material. Therefore, the critical angle is related only to the real part of the complex refractive index, which can be calculated as follows.

$$n = 1 - \delta = \cos(\theta_c) \fallingdotseq 1 - \frac{\theta_c^2}{2} \qquad (4)$$

$$\theta_c \fallingdotseq \sqrt{2\delta} \qquad (5)$$

Since the δ value includes the density information of the sample, which can be calculated from the critical angle value of the incident X-ray beam. In our data, the critical angle is 0.35°, which gives the density of SBDDDVE as 1.58 g/cm^3.

<u>Conformal coating on complex structure</u>

In the EDS spectra from the cross-sectional images in **Fig. S2**, bare stainless steel mesh shows only a trace amount of sulfur, while the stainless steel mesh coated with 200 nm-thick SBDDVE shows 9.43 wt% sulfur content at the side of the mesh fiber, which indicates deposition of SCP is accomplished.

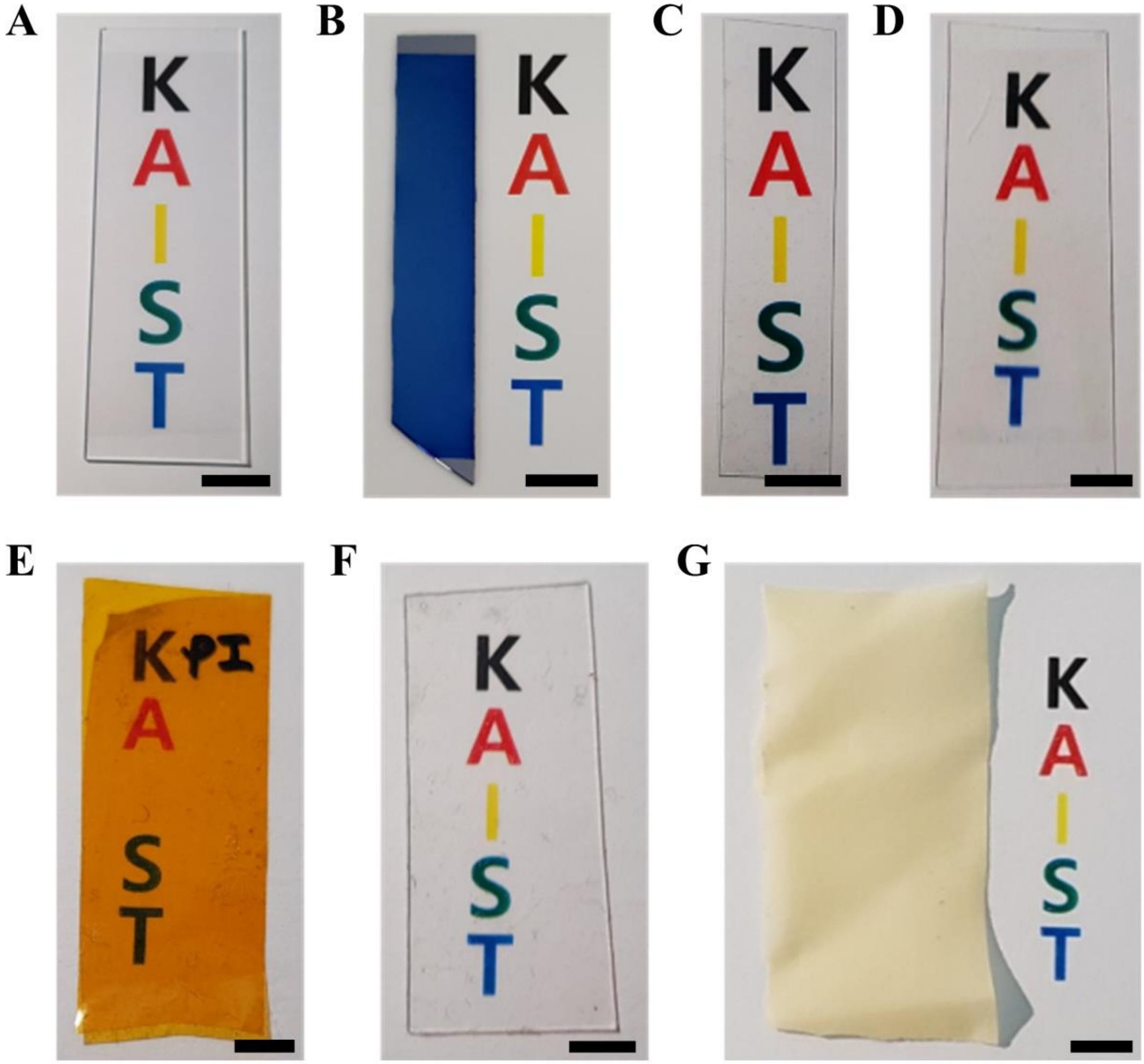

Fig. S1. SCP films on various substrates. Digital camera images of the colorless poly(sulfur-*co*-1,4-butanediol divinyl ether) (SBDDVE) films (thickness = 110 nm), deposited on (**A**) glass, (**B**) silicon wafer, (**C**) polyethylene terephthalate (PET), (**D**) polyethylene naphthalate (PEN), (**E**) polyimide (PI), (**F**) polydimethyl siloxane (PDMS), and (**G**) latex. (Scale bar : 1cm) Photo credit: Wontae Jang (Korea Advanced Institute of Science and Technology).

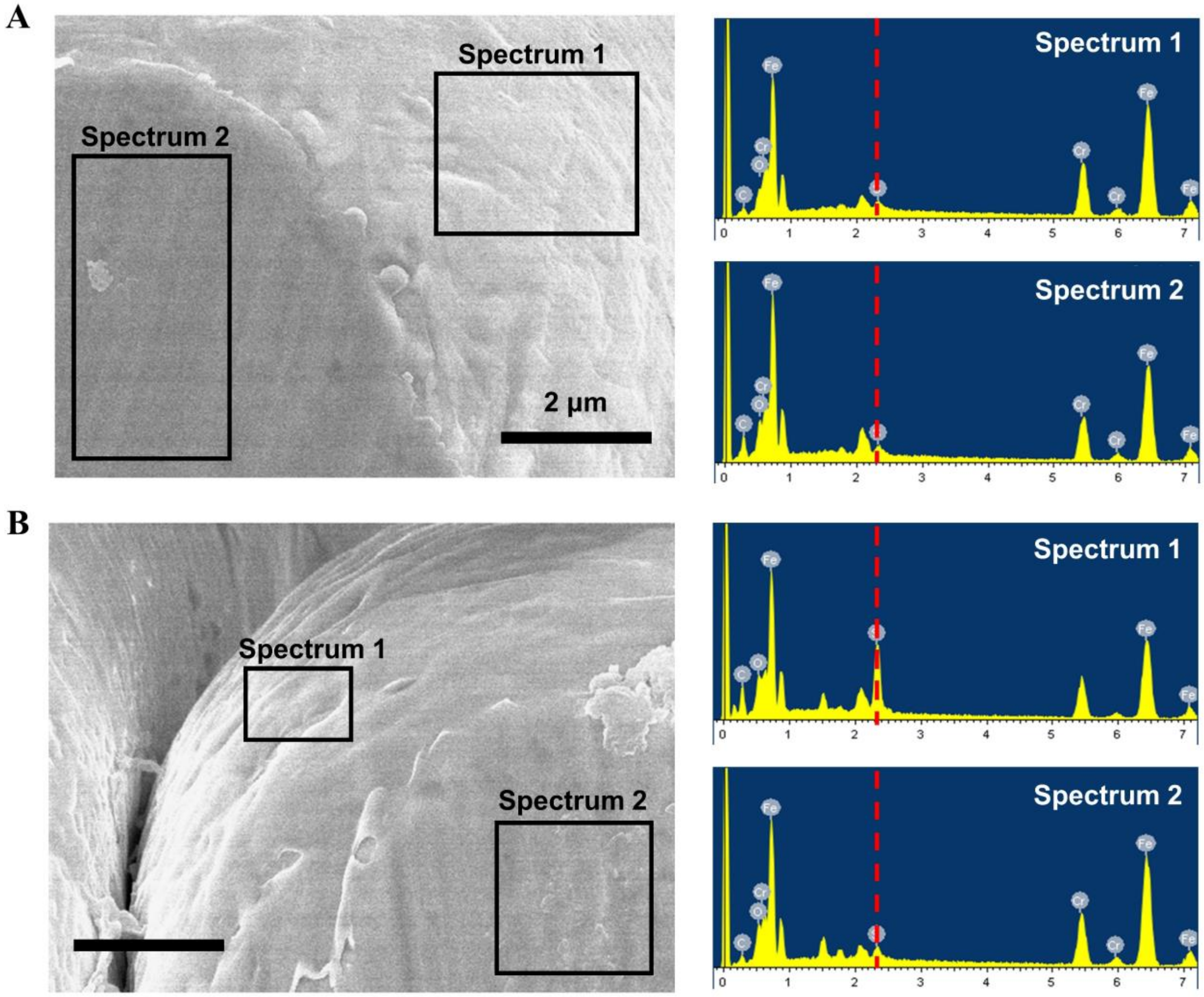

Fig. S2. Cross-sectional scanning electron microscope (SEM) image and energy dispersive spectroscopy (EDS) scan spectra with sulfur atom peaks (red dash line) of the stainless steel mesh coated with the sulfur-containing polymer (SCP) film (Spectrum 1) and the non-coated area (Spectrum 2) of (**A**) before and (**B**) after the 200 nm SBDDVE film deposition on the stainless steel mesh.

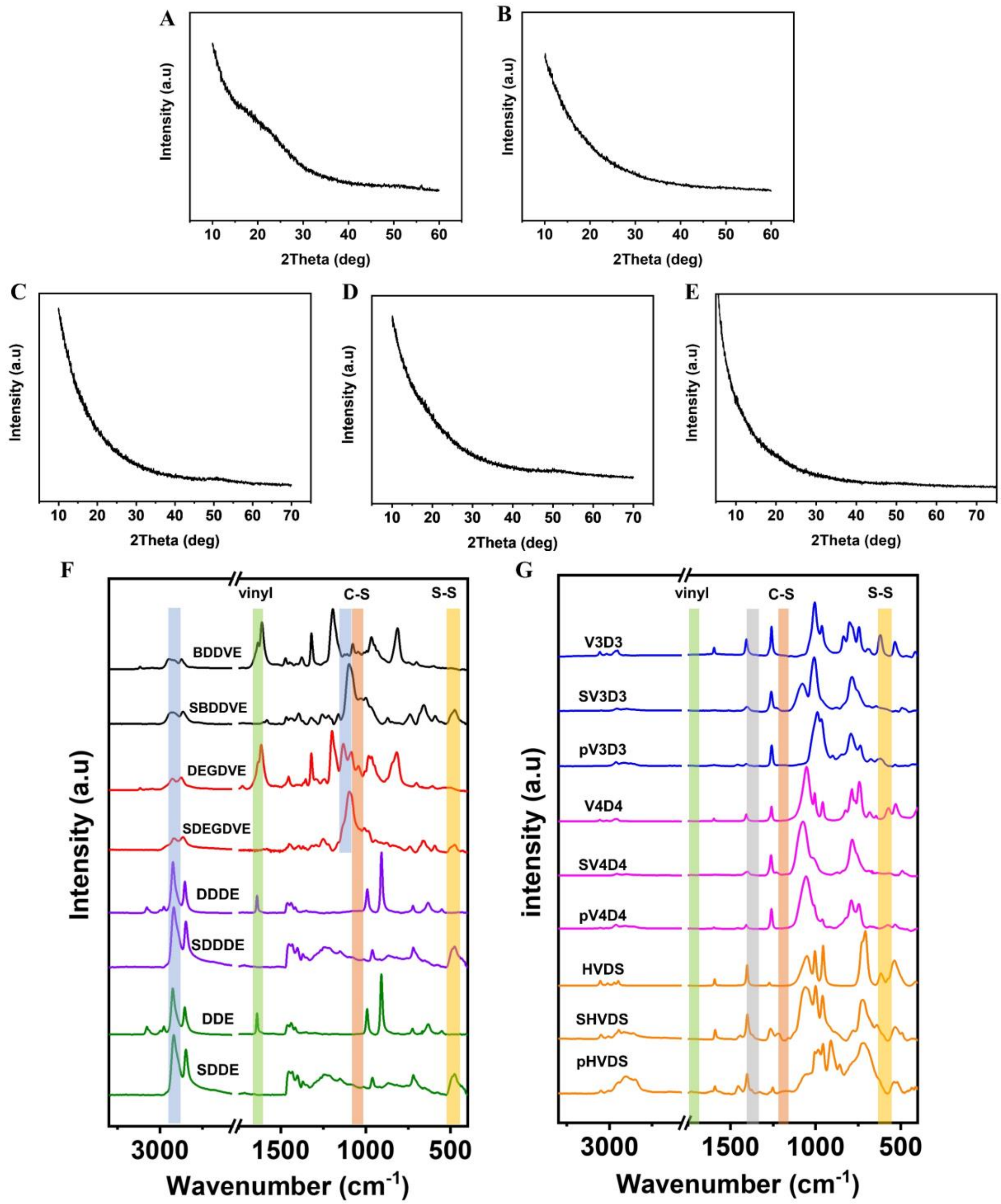

Fig. S3. X-ray diffraction (XRD) spectra of (**A**) SBDDVE film with 61.64 wt% and (**B**) 66.82 wt% of sulfur contents; (**C**) SV4D4, (**D**) SV3D3, (**E**) SHVDS, deposited by sCVD, and **Fourier transform infrared (FTIR) spectra** of **(F)** 1, 4-butanediol divinyl ether (BDDVE), di(ethylene glycol)divinyl ether (DEGDVE), 1,11-dodecadiene (DDDE), 1,9-decadiene(DDE), and the SCPs of poly(sulfur-co-1,4-butanediol divinyl ether) (SBDDVE), poly(sulfur-co-di(ethylene glycol)divinyl ether) (SDEGDVE), poly(sulfur-co-1,11-dodecadiene) (SDDDE), poly(sulfur-co-1,9-decadiene) (SDDE) synthesized by sCVD, **(G)** 1,3,5-trivinyl-1,3,5-trimethylcyclotrisiloxane(V3D3), 1,3,5,7-tetravinyl-1,3,5,7-tetramethylcyclotetrasiloxane

(V4D4), hexavinyldisiloxane (HVDS) monomer, and their corresponding polymers of poly(1,3,5-trivinyl-1,3,5-trimethylcyclotrisiloxane) (pV3D3), poly(1,3,5,7-tetravinyl-1,3,5,7-tetramethyl cyclotetrasiloxane) (pV4D4), poly(hexavinyldisiloxane) (pHVDS), and the SCPs of poly(sulfur-co-di(ethylene glycol)divinyl ether) (SDEGDVE), poly(sulfur-co-1,3,5-trivinyl-1,3,5-trimethylcyclotrisiloxane) (SV3D3), poly(sulfur-co-1,3,5,7-tetravinyl-1,3,5,7-tetramethylcyclotetrasiloxane) (SV4D4), and poly(sulfur-co-hexavinyldisiloxane) (SHVDS), synthesized by sCVD, where blue area at 1100, 2900 cm^{-1} represent -C-O-C- and -C-H stretching peaks, respectively, and gray area at 1260 cm^{-1} represents $Si\text{-}CH_3$ peak.

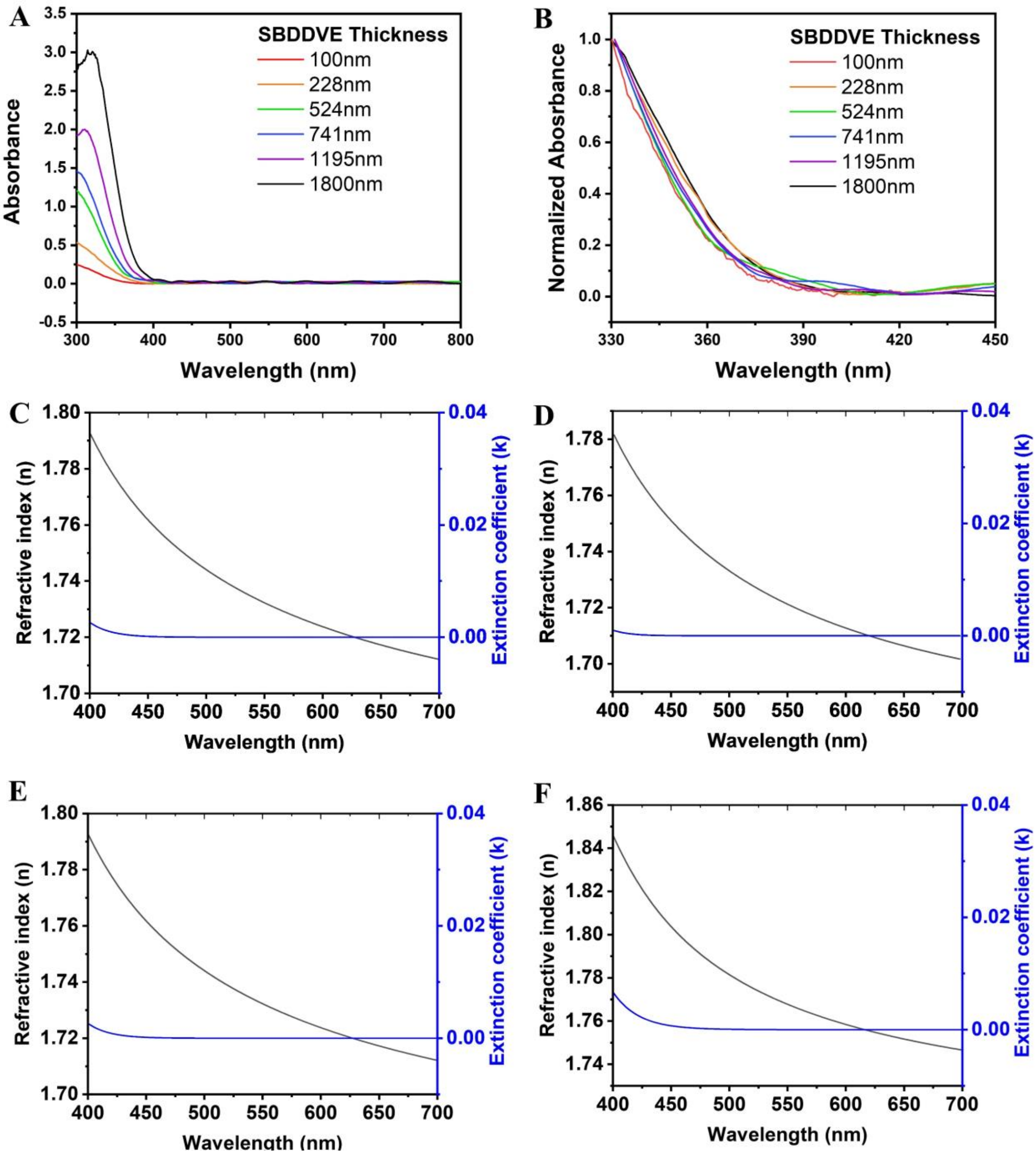

Fig. S4. UV-Vis absorbance (**A**) and normalized UV-Vis absorbance (**B**) spectra of SBDDVE films of varying thickness obtained from sCVD, and the refractive index (*n*) and extinction coefficient (*k*) values of (**C**) SV3D3, (**D**) SV4D4, (**E**) SDDDE, (**F**)SDDE obtained by ellipsometry measurement.

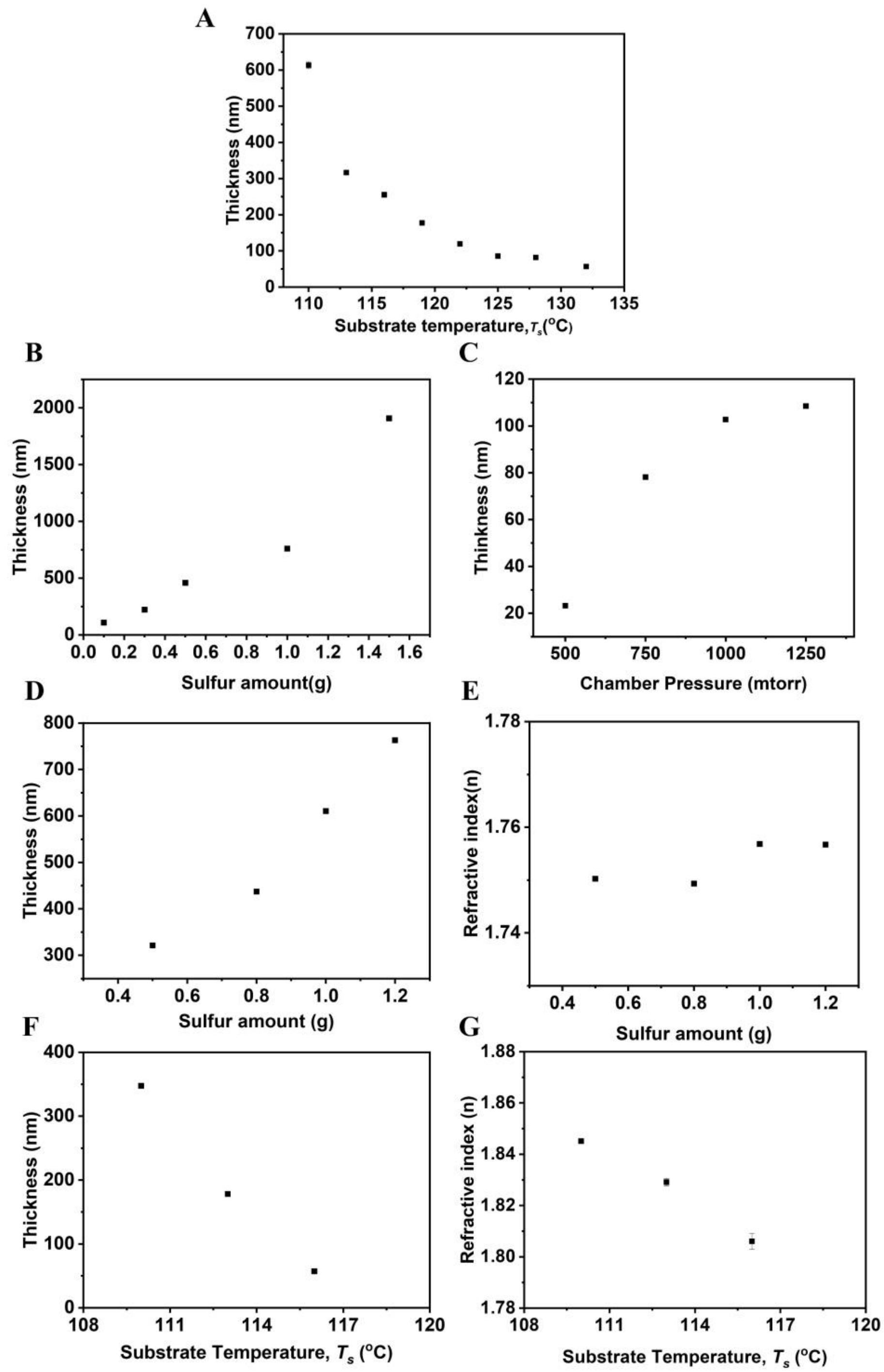

Fig. S5. Thickness variation of SBDDVE film with respect to (**A**) substrate temperatur (T_S) (**B**) the sulfur loading amount (with the fixed chamber pressure of 1000 mTorr and substrate temperature (T_s) = 110 °C), (**C**) the chamber pressure (with the fixed sulfur amount 0.1 g and T_s = 110 °C), **(D)** Thickness, (**E**) refractive index variation of SBDDVE film with respect to sulfur loading amount (with the fixed chamber pressure of 1000 mTorr and T_s = 110 °C) with 120 min reaction time, **(F)** thickness, (**G**) refractive index variation of the substrate temperature (with the fixed sulfur loading amount of 0.3 g and the process pressure of 1000 mTorr).

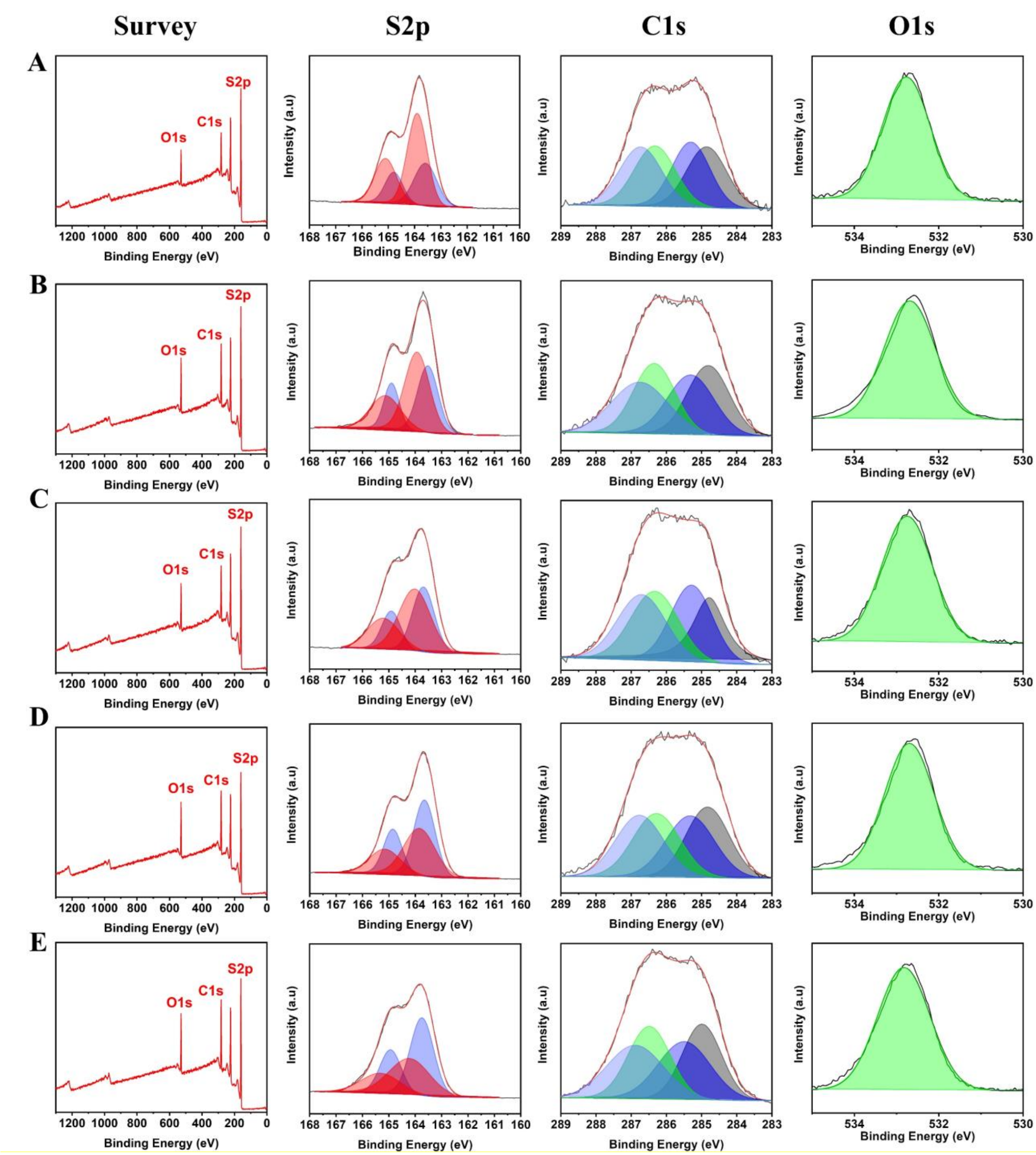

Fig. S6. X-ray photoelectron spectroscopy (XPS) survey spectra and deconvoluted S2p (left), C1s (center), O1s (right) XPS high resolution scan spectra of SBDDVE films with various sulfur contents of (**A**) 71.90 wt%, (**B**) 68.82 wt%, (**C**) 66.86 wt%, (**D**) 63.58 wt%, and (**E**) 61.69 wt%. Deconvoluted spectra are colored with light blue for S-C-O, green for C-O, blue for C-S, and grey for C-C in C1s XPS high resolution spectra, blue for C-S and red for S-S, respectively, in S2p XPS high resolution spectra, and green as C-O in O1s XPS high resolution spectra.

Table S1. Comparison of SCPs from sCVD with those synthesized by other methods. Tristan S. Kleine (University of Arizona) and Wontae Jang (Korea Advanced Institute of Science and Technology).

Material		$n_{632.8nm}$	Color	Notes	Ref
	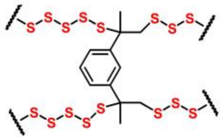	1.87	Yellow/ Red	▪ Synthesized by inverse vulcanization ▪ Must use olefin monomer miscible with elemental sulfur ▪ A strong absorption in visible region ▪ Hard to mold into thin film due to the lack of solubility in common organic solvents.	1
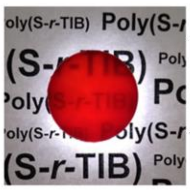	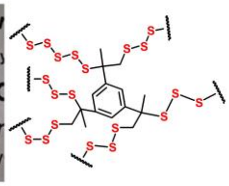	1.83	Orange/ Red	▪ Synthesized by inverse vulcanization ▪ Use of sulfur and olefin comonomer with tri-vinyl groups ▪ A strong absorption in visible region	6
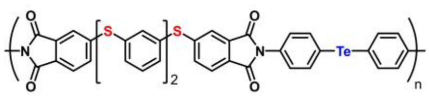		1.78	Yellow	▪ Multi-step synthesis. ▪ Tellurium was used to maximize the refractive index. ▪ A strong absorption in visible region	39
	**This study**	> 1.90	Colorless	▪ One-step sCVD in vapor phase. ▪ No limit in monomer selection. ▪ Fully transparent in whole visible region. ▪ Film thickness and refractive index properties can be controlled in systematic manner. ▪ Extremely high refractive index larger than 1.9.	

Table S2. Refractive index from ellipsometry measurement, and calculated Abbe's number (v_D) of the SBDDVE films with two different refractive index, SDDDE, SDDE, SV3D3, and SV4D4 synthesized by sCVD.

Polymer	$n_{632.8}$	$n_{656.3}$	$n_{589.3}$	$n_{486.1}$	v_D
SBDDVE	1.915	1.910	1.926	1.973	14.698
	1.726	1.724	1.732	1.755	23.613
SDDDE	1.719	1.717	1.725	1.748	23.387
SDDE	1.754	1.751	1.760	1.787	21.111
SV3D3	1.729	1.726	1.737	1.767	17.976
SV4D4	1.708	1.706	1.714	1.738	22.313

Table S3. XPS survey scan quantitative result of SBDDVE films with various sulfur weight % (wt%), copolymer ratio, and S-S/S-C bond ratio.

Sulfur wt%	Atomic %			Copolymer ratio	S-S/S-C ratio
	S	C	O	S_8 : BDDVE	
71.90	52.81	37.24	9.95	1.42 : 1	1.84
68.82	48.48	39.63	11.88	1.22 : 1	1.45
66.86	46.21	41.31	12.49	1.12 : 1	1.24
63.58	43.23	44.68	12.09	0.97 : 1	0.94
61.69	41.46	46.44	12.09	0.89 : 1	0.79

*** Considered Molecular weight of S_8 is 256.52, and BDDVE is 142.2**

Table S4. XPS S2p, C1s high resolution scan quantitative result of SBDDVE films with various sulfur weight % (wt%), calculated S-C bond ration in total polymer, and S-S/S-C bond ratio

Sulfur wt%	S2p deconvoluted area (a.u.)				S-C bond ratio in total polymer (%)	S-S/S-C ratio
	C-S $2p_{1/2}$	C-S $2p_{3/2}$	S-S $2p_{1/2}$	S-S $2p_{3/2}$		
71.90	8323.85	16647.69	16324.03	32648.06	17.83	1.96
68.82	13192.70	26385.40	18700.00	37400.00	20.05	1.42
66.86	13628.79	27257.58	18591.42	37182.83	19.54	1.36
63.58	15622.28	31244.56	14174.77	28349.55	22.66	0.91
61.69	16201.22	32402.44	12762.19	25524.38	23.19	0.79

Sulfur wt%	C1s deconvoluted area (a.u.)				S-C bond ratio in total polymer (%)
	S-C-O	C-O	C-S	C-C	
71.90	7341.494	7381.83	7229.488	7255.087	18.58
68.82	12404.24	11721.76	12283.53	12036.01	20.20
66.86	12631.49	13623.93	13757.76	13140.88	20.51
63.58	14222.58	13890.16	13877.22	13602.36	22.58
61.69	13843.02	14036.51	14196.76	14008	23.22

REFERENCES AND NOTES

1. J. J. Griebel, S. Namnabat, E. T. Kim, R. Himmelhuber, D. H. Moronta, W. J. Chung, A. G. Simmonds, K.-J. Kim, J. van der Laan, N. A. Nguyen, E. L. Dereniak, M. E. Mackay, K. Char, R. S. Glass, R. A. Norwood, J. Pyun, New infrared transmitting material via inverse vulcanization of elemental sulfur to prepare high refractive index polymers. *Adv. Mater.* **26**, 3014–3018 (2014).

2. L. E. Anderson, T. S. Kleine, Y. Zhang, D. D. Phan, S. Namnabat, E. A. LaVilla, K. M. Konopka, L. Ruiz Diaz, M. S. Manchester, J. Schwiegerling, R. S. Glass, M. E. Mackay, K. Char, R. A. Norwood, J. Pyun, Chalcogenide hybrid inorganic/organic polymers: Ultrahigh refractive index polymers for infrared imaging. *ACS Macro Lett.* **6**, 500–504 (2017).

3. T. Higashihara, M. Ueda, Recent progress in high refractive index polymers. *Macromolecules* **48**, 1915–1929 (2015).

4. Y. Suzuki, T. Higashihara, S. Ando, M. Ueda, Synthesis of high refractive index poly (thioether sulfone) s with high Abbe's number derived from 2,5-is (sulfanylmethyl)-l,4-dithiane. *Polymer J.* **41**, 860–865 (2009).

5. Y. Suzuki, T. Higashihara, S. Ando, M. Ueda, Synthesis and characterization of high refractive index and high Abbe's number poly(thioether sulfone)s based on tricyclo [5.2.1.$0^{2,6}$] decane moiety. *Macromolecules* **45**, 3402–3408 (2012).

6. T. S. Kleine, N. A. Nguyen, L. E. Anderson, S. Namnabat, E. A. LaVilla, S. A. Showghi, P. T. Dirlam, C. B. Arrington, M. S. Manchester, J. Schwiegerling, R. S. Glass, K. Char, R. A. Norwood, M. E. Mackay, J. Pyun, High refractive index copolymers with improved thermomechanical properties via the inverse vulcanization of sulfur and 1,3,5-triisopropenylbenzene. *ACS Macro Lett.* **5**, 1152–1156 (2016).

7. J. J. Griebel, N. A. Nguyen, S. Namnabat, L. E. Anderson, R. S. Glass, R. A. Norwood, M. E. Mackay, K. Char, J. Pyun, Dynamic covalent polymers via inverse vulcanization of elemental sulfur for healable infrared optical materials. *ACS Macro Lett.* **4**, 862–866 (2015).

8. W. J. Chung, J. J. Griebel, E. T. Kim, H. Yoon, A. G. Simmonds, H. J. Ji, P. T. Dirlam, R. S. Glass, J. J. Wie, N. A. Nguyen, B. W. Guralnick, J. Park, A. Somogyi, P. Theato, M. E. Mackay, Y.-E. Sung, K.

Char, J. Pyun, The use of elemental sulfur as an alternative feedstock for polymeric materials. *Nat. Chem.* **5**, 518–524 (2013).

9. J. J. Griebel, R. S. Glass, K. Char, J. Pyun, Polymerizations with elemental sulfur: A novel route to high sulfur content polymers for sustainability, energy and defense. *Prog. Polym. Sci.* **58**, 90–125 (2016).

10. A. V. Tobolsky, A. Eisenberg, Equilibrium polymerization of sulfur. *J. Am. Chem. Soc.* **81**, 780–782 (1959).

11. A. V. Tobolsky, Polymeric sulfur and related polymers. *J. Polymer Sci.* **12**, 71–78 (1966).

12. T. S. Kleine, R. S. Glass, D. L. Lichtenberger, M. E. Mackay, K. Char, R. A. Norwood, J. Pyun, 100th anniversary of macromolecular science viewpoint: High refractive index polymers from elemental sulfur for infrared thermal imaging and optics. *ACS Macro Lett.* **9**, 245–259 (2020).

13. T. S. Kleine, T. Lee, K. J. Carothers, M. O. Hamilton, L. E. Anderson, L. Ruiz Diaz, N. P. Lyons, K. R. Coasey, W. O. Parker Jr., L. Borghi, M. E. Mackay, K. Char, R. S. Glass, D. L. Lichtenberger, R. A. Norwood, J. Pyun, Infrared fingerprint engineering: A molecular-design approach to long-wave infrared transparency with polymeric materials. *Angew. Chem. Int. Ed.* **58**, 17656–17660 (2019).

14. A. M. Coclite, P. Lund, R. Di Mundo, F. Palumbo, Novel hybrid fluoro-carboxylated copolymers deposited by initiated chemical vapor deposition as protonic membranes. *Polymer* **54**, 24–30 (2013).

15. M. J. Kwak, M. S. Oh, Y. Yoo, J. B. You, J. Kim, S. J. Yu, S. G. Im, Series of liquid separation system made of homogeneous copolymer films with controlled surface wettability. *Chem. Mater.* **27**, 3441–3449 (2015).

16. X. Wu, J. A. Smith, S. Petcher, B. Zhang, D. J. Parker, J. M. Griffin, T. Hasell, Catalytic inverse vulcanization. *Nat. Commun.* **10**, 647 (2019).

17. I. Gomez, D. Mecerreyes, J. A. Blazquez, O. Leonet, H. Ben Youcef, C. Li, J. L. Gómez-Cámer, O. Bondarchuk, L. Rodriguez-Martine, Inverse vulcanization of sulfur with divinylbenzene: Stable and easy processable cathode material for lithium-sulfur batteries. *J. Power Sources* **329**, 72–78 (2016).

18. D. J. Parker, H. A. Jones, S. Petcher, L. Cervini, J. M. Griffin, R. Akhtar, T. Hasell, Low cost and renewable sulfur-polymers by inverse vulcanisation, and their potential for mercury capture. *J. Mater. Chem. A* **5**, 11682–11692 (2017).

19. Y. Zhao, F. Yin, Y. Zhang, C. Zhang, A. Mentbayeva, N. Umirov, H. Xie, Z. Bakenov, A free-standing sulfur/nitrogen-doped carbon nanotube electrode for high-performance lithium/sulfur batteries. *Nanoscale Res. Lett.* **10**, 450 (2015).

20. Z. Sun, M. Xiao, S. Wang, D. Han, S. Song, G. Chen, Y. Meng, Sulfur-rich polymeric materials with semi-interpenetrating network structure as a novel lithium–sulfur cathode. *J. Mater. Chem. A* **2**, 9280–9286 (2014).

21. H. Ding, J.-S. Wei, H.-M. Xiong, Nitrogen and sulfur co-doped carbon dots with strong blue luminescence. *Nanoscale* **6**, 13817–13823 (2014).

22. B. C. Smith, The CO bond III: Ethers by a knockout. *Spectroscopy* **32**, 22–26 (2017).

23. W. S. O'Shaughnessy, M. Gao, K. K. Gleason, Initiated chemical vapor deposition of trivinyltrimethylcyclotrisiloxane for biomaterial coatings. *Langmuir* **22**, 7021–7026 (2006).

24. H. Moon, H. Seong, W. C. Shin, W.-T. Park, M. Kim, S. Lee, J. H. Bong, Y.-Y. Noh, B. J. Cho, S. Yoo, S. G. Im, Synthesis of ultrathin polymer insulating layers by initiated chemical vapour deposition for low-power soft electronics. *Nat. Mater.* **14**, 628–635 (2015).

25. D. Braun, F. Hu, Polymers from non-homopolymerizable monomers by free radical processes. *Prog. Polym. Sci.* **31**, 239–276 (2006).

26. J. Choi, J. Yoon, M. J. Kim, K. Pak, C. Lee, H. Lee, K. Jeong, K. Ihm, S. Yoo, B. J. Cho, H. Lee, S. G. Im, Spontaneous generation of a molecular thin hydrophobic skin layer on a sub-20 nm, high-*k* polymer dielectric for extremely stable organic thin-film transistor operation. *ACS Appl. Mater. Interfaces* **11**, 29113–29123 (2019).

27. G. Aresta, J. Palmans, M. C. van de Sanden, M. Creatore, Initiated-chemical vapor deposition of organosilicon layers: Monomer adsorption, bulk growth, and process window definition. *J. Vac. Sci. Technol. A* **30**, 041503 (2012).

28. M. B. Sassin, J. W. Long, J. M. Wallace, D. R. Rolison, Routes to 3D conformal solid-state dielectric polymers: Electrodeposition *versus* initiated chemical vapor deposition. *Mater. Horiz.* **2**, 502–508 (2015).

29. A. Abdul Razzaq, Y. Yao, R. Shah, P. Qi, L. Miao, M. Chen, X. Zhao, Y. Peng, Z. Deng, High-performance lithium sulfur batteries enabled by a synergy between sulfur and carbon nanotubes. *Energy Storage Mater.* **16**, 194–202 (2019).

30. J. Ye, F. He, J. Nie, Y. Cao, H. Yang, X. Ai, Sulfur/carbon nanocomposite-filled polyacrylonitrile nanofibers as a long life and high capacity cathode for lithium–sulfur batteries. *J. Mater. Chem. A* **3**, 7406–7412 (2015).

31. H. Kim, J. Lee, H. Ahn, O. Kim, M. J. Park, Synthesis of three-dimensionally interconnected sulfur-rich polymers for cathode materials of high-rate lithium–sulfur batteries. *Nat. Commun.* **6**, 7278 (2015).

32. B. Meyer, K. Spitzer, Extended Hückel calculations on the color of sulfur chains and rings. *J. Phys. Chem.* **76**, 2274–2279 (1972).

33. B. Meyer, Elemental sulfur. *Chem. Rev.* **76**, 367–388 (1976).

34. R. Steudel, Y. Steudel, M. W. Wong, Speciation and thermodynamics of sulfur vapor, in *Elemental Sulfur and Sulfur-Rich Compounds I* (Springer, 2003), pp. 117–134.

35. S. J. Yoon, K. Pak, T. Nam, A. Yoon, H. Kim, S. G. Im, B. J. Cho, Surface-localized sealing of porous ultralow-*k* dielectric films with ultrathin (< 2 nm) polymer coating. *ACS Nano* **11**, 7841–7847 (2017).

36. Y. I. Lee, N. J. Jeon, B. J. Kim, H. Shim, T.-Y. Yang, S. I. Seok, J. Seo, S. G. Im, A low-temperature thin-film encapsulation for enhanced stability of a highly efficient perovskite solar cell. *Adv. Energy Mater.* **8**, 1701928 (2018).

37. S. J. Yu, K. Pak, M. J. Kwak, M. Joo, B. J. Kim, M. S. Oh, J. Baek, H. Park, G. Choi, D. H. Kim, J. Choi, Y. Choi, J. Shin, H. Moon, E. Lee, S. G. Im, Initiated chemical vapor deposition: A versatile tool for various device applications. *Adv. Eng. Mater.* **20**, 1700622 (2018).

38. M. Yasaka, X-ray thin-film measurement techniques V. X-ray reflectivity measurement. *Rigaku J.* **26**, 1–9 (2010).

39. H. Kim, B.-C. Ku, M. Goh, H. C. Ko, S. Ando, N.-H. You, Synergistic effect of sulfur and chalcogen atoms on the enhanced refractive indices of polyimides in the visible and near-infrared regions. *Macromolecules*, **52**, 827–834 (2019).